Improving Pedestrian Dead Reckoning Accuracy for Smartphone Users through GNSS/PDR Integrated Navigation

Ryoya Shiraiwa
Department of Electrical and Electronic Engineering
Ritsumeikan University
Shiga, Japan
re0139fs@ed.ritsumei.ac.jp

Fumiya Odai
Department of Electrical and Electronic Engineering
Ritsumeikan University
Shiga, Japan
re0120ik@ed.ritsumei.ac.jp

Yukihiro Kubo
Department of Electrical and Electronic Engineering
Ritsumeikan University
Shiga, Japan
ykubo@se.ritsumei.ac.jp

***Abstract*—In recent years, location-based services (LBS) have attracted much attention because of increasing smartphone users. The technology mainly used for estimating position of smartphone users is the global navigation satellite system (GNSS). However, the satellite positioning has demerit it cannot provide accurate position information in environments such as indoors or near buildings. Therefore, we focus on the pedestrian dead reckoning (PDR), which estimates the pedestrian position using the sensors in the terminal. The positioning by PDR needs to take into account the walking characteristics of the pedestrian individually. This paper proposes a method to adaptively estimate the parameters for pedestrians to improve the accuracy of positioning by PDR.**

***Index Terms*—LBS, smartphone, PDR, GNSS**

I. Introduction

The number of smartphone users has been steadily growing and the demand for location-based services (LBS) is increasing. The technology mainly used for estimating position of smartphone users is the global navigation satellite system (GNSS). However, the satellite positioning has demerit it cannot provide accurate position information because the number of observable satellites decrease in the situation such as near buildings, trees, and other obstacles. Other method besides the satellite positioning includes the wireless fidelity (Wi-Fi) positioning [1] and the Bluetooth low energy (BLE) positioning [2]. The Wi-Fi positioning and the BLE positioning are restricted to a specific location, but pedestrian dead reckoning (PDR) [3] is a method that can be completed only with a terminal. Compared to Wi-Fi positioning and BLE positioning, PDR has high versatility because it can be used anywhere and using sensors of terminal. However, it is difficult to estimate the position of pedestrian by PDR because PDR needs to take into account the walking characteristics of the pedestrian individually. On the other hand, GNSS has high versatility because it can be used in most smartphones. Therefore, we focused on improving the accuracy of PDR using GNSS, which can be easily used in a lot of smartphones.

PDR is to estimate position of pedestrian by using sensors equipped (inertial measurement unit (IMU), magnetic sensor, pressure sensor, etc.). There are a lot of research on PDR, in which a common approach involves estimating the position of pedestrian using the following three steps: (a) walking detection, (b) stride length estimation, and (c) heading angle estimation.

The walking detection is mainly implemented using an acceleration sensor. During walking, the measured acceleration shows a cyclical characteristic, which can be utilized to detect walking by comparing with a threshold given in advance [4], [5].

The stride length estimation includes a method that uses experimentally determined parameters or models [6]–[8]. Consequently, the accuracy of PDR strongly depends on the parameters and models applied.

Most of the studies on the heading angle estimation use gyro sensors [5], [9], so there is concern about the accumulation of errors.

The previous studies of stride length estimation have used experimentally determined parameters and models by assuming that people perform the specific walking motion. However, it can be considered that the characteristic of the walking motion depends on individual pedestrian's age, height, and so on, there is no general parameters and models suitable for all people and walking motions. Also, the previous studies of heading angle estimation depend on how the pedestrian holds the smartphone and the pedestrian walks.

Therefore, we have been motivated to develop the PDR system that can adaptively estimate the parameters describing the characteristic of the individual pedestrian's walking motion and how the pedestrian holds the smartphone.

There also exist a lot of literature on the integrated navigation using GNSS/PDR, e.g. [5], [9]–[13]. However, it has been pointed out that the PDR used in these related studies does not sufficiently take into account differences among pedestrians. Therefore, we propose a method that realizes parameter estimation suitable for walking motion including

979-8-3503-0219-6/23/$31.00 ©2023 IEEE

how the pedestrian holds the smartphone by GNSS/PDR integrated navigation.

II. Pedestrian Dead Reckoning

In this paper, we consider the human movement caused by walking, therefore, PDR in this study consists of the following three steps: walking detection, stride length estimation, and heading angle estimation.

A. Pedestrian position model

Fig. 1 shows the east-north-up (ENU) coordinate system [14] for the GNSS/PDR integrated navigation processing. $\boldsymbol{r}_k(=[e_k,\ n_k]^{\mathrm{T}})$ is pedestrian's position at the k-th step detected. $\boldsymbol{r}_0$ is the starting point. L_k and ψ_k are pedestrian's stride length and heading angle at the k-th step respectively. Then the pedestrian's position can be modeled as

$$e_k = e_{k-1} + L_{k-1}\sin\psi_{k-1} + w_k^e \tag{1}$$

$$n_k = n_{k-1} + L_{k-1}\cos\psi_{k-1} + w_k^n \tag{2}$$

where $w_k^e,\ w_k^n$ are Gaussian white noises. Also, we assume that heading angle and direction of travel in this paper.

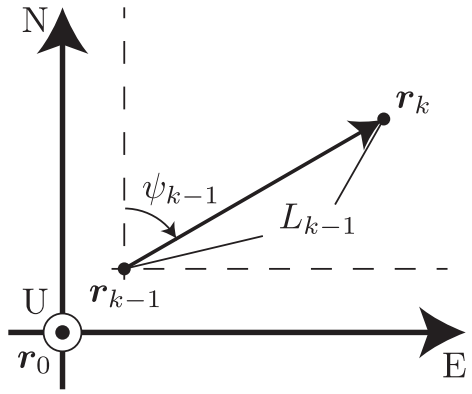

Fig. 1. Pedestrian position coordinate system

B. Walking detection

The walking detection is implemented by using A_n. A_n is the norm of the three dimensional acceleration obtained by the smartphone as follows.

$$A_n = \sqrt{A_{x,n}^2 + A_{y,n}^2 + A_{z,n}^2} - g \tag{3}$$

where the subscript n is the index of data, g is the gravitational acceleration, and $x,\ y,\ z$ are corresponding to three dimensional axses. In addition, the noise is removed by applying the moving average filter [15] to A_n. $\hat{A}_n$ obtained by applying moving average filter to A_n can be expressed as follows.

$$\hat{A}_n = \frac{1}{M}\sum_{m=0}^{M-1} A_{n-m} \tag{4}$$

where M is the array dimension, and let $n-m$ satisfy $n-m \geq 1$. M can be expressed as follows.

$$M = \frac{0.443 f_s}{f_c} \tag{5}$$

where f_s is the sampling frequency, f_c is the cut off frequency. f_s is calculated from the actual sensors output. Assuming that walking is generally one or two steps per second, let f_c be 3 Hz. M is rounded to an integer value. In the following, in order to simplify the notation, the averaged acceleration $\hat{A}_n$ is expressed as A_n.

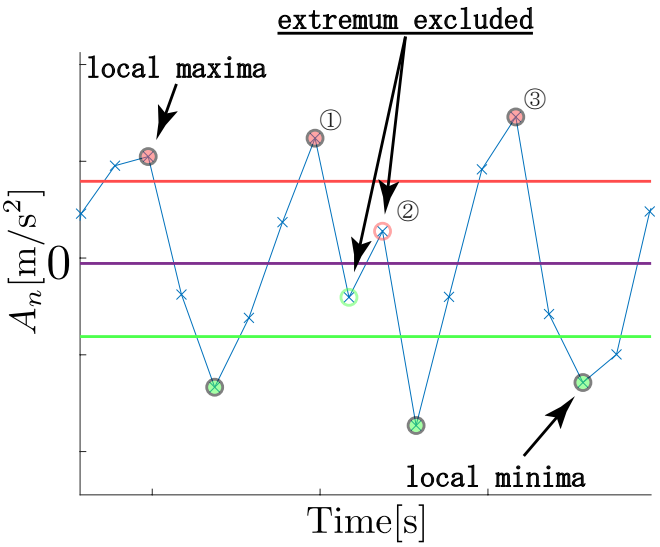

Fig. 2. Pedestrian position coordinate system

Fig. 2 shows an example of the change in A_n due to walking motion. The walking detection is performed by zero crossing method [16]. Within the interval of one step, A_n gives local maxima and minima, respectively. To remove the false walking detection, this study set thresholds for each extremum. $0.6\ \mathrm{m/s^2}$ is set as the threshold for the maximum value, and $-0.6\ \mathrm{m/s^2}$ is set as the threshold for the minimum value. Extremum that do not satisfy these thresholds are not treated as extreme values. Furthermore, the time difference between the local minima and the local maxima shold be less than 1.5 seconds. If it exceeds 1.5 seconds, they are ignored in the walking detection. 1.5 seconds is based on the assumption that pedestrians do not take 3 steps in 1 second. The zero crossing points are defined by timing when A_n fell below 0.

Examples of zero crossing points are shown by ①, ②, ③, and ④ in Fig. 2. Since the walking step is detected only when the thresholds and time interval are satisfied, the period between ①→② and ③→④ are considered as the walking period. In addition, since the threshold for extreme values is not satisfied during the period from ②→③, it is not treated as a walking periods. In this way, walking detection is performed by using acceleration sensor.

C. Stride length estimation

The k-th stride length L_k can be considered to depend on the reciprocal of the time taken for the k-th step f_k. Therefore, we express L_k as follows [18].

$$L_k = \beta_k + \gamma_k f_k \tag{6}$$

where $\beta_k,\ \gamma_k$ are the coefficient parameters. f_k is calculated according to the above-mentioned walking detection. For example, if ①→② in Fig. 2 is the k-th step, f_k is represented by $1/(T_2 - T_1)$, where T_1 is the time at ① and T_2 is the time at ② time. By estimating β_k and γ_k for each pedestrian, we can adaptively perform PDR for individual pedestrian.

$\beta_k,\ \gamma_k$ are estimated by GNSS/PDR integrated navigation, which will be described in Section Ⅲ.

D. Heading angle estimation

The k-th heading angle ψ_k is estimated by magnetic sensor and estimating attitude of the smartphone. We express ψ_k as follows.

$$\psi_k = \psi_k^{mag} + \alpha_k \tag{7}$$

where ψ_k^{mag} is measured heading angle by magnetic sensor, α_k is the misalignment between the direction of travel and the smartphone. Calculation of ψ_k^{mag} requires attitude estimation of the smartphone.

The attitude of the smartphone is estimated by Kalman filter (KF) [17]. The state-space model for KF can be expressed as follows.

$$\begin{bmatrix}\phi_{i+1}\\ \theta_{i+1}\end{bmatrix} = \begin{bmatrix}\phi_i\\ \theta_i\end{bmatrix} + \begin{bmatrix}w_i^{\phi}\\ w_i^{\theta}\end{bmatrix} \tag{8}$$

$$\begin{bmatrix}\phi_i^{acc}\\ \theta_i^{acc}\\ \phi_i^{gyr}\\ \theta_i^{gyr}\end{bmatrix} = \begin{bmatrix}\phi_i\\ \theta_i\\ \phi_i\\ \theta_i\end{bmatrix} + \begin{bmatrix}v_i^{\phi,acc}\\ v_i^{\theta,acc}\\ v_i^{\phi,gyr}\\ v_i^{\theta,gyr}\end{bmatrix} \tag{9}$$

where the subscript i is the index number of the time when the IMU outputs its data, $\phi_i,\ \theta_i$ are the roll and pitch angle of the smartphone, the superscripts $acc,\ gyr$ mean the corresponding values based on acceleration sensor, gyro sensor respectively. The noises $w_i^{\phi},\ w_i^{\theta},\ v_i^{\phi,acc},\ v_i^{\theta,acc},\ v_i^{\phi,gyr},\ v_i^{\theta,gyr}$ are assumed to be zero mean Gaussian white noises. ϕ_i^{acc} and θ_i^{acc} are uniquely determined when the only acceleration applied to the sensor is gravitational acceleration. ϕ_i^{gyr} and θ_i^{gyr} are estimated by setting the initial values to ϕ_0^{acc} and θ_0^{acc}, respectively, and calculating the amount of change from that time using the gyro sensor values along each axis. The distribution of each noise is experimentally designated as Table I.

TABLE I
NOISE DISTRIBUTIONS OF SMARTPHONE ATTITUDE ESTIMATION

w_i^{ϕ}	$N(0,\ 0.0873^2)$
w_i^{θ}	$N(0,\ 0.0873^2)$
$v_i^{\phi,acc}$	$N(0,\ 0.0524^2)$
$v_i^{\theta,acc}$	$N(0,\ 0.0524^2)$
$v_i^{\phi,gyr}$	$N(0,\ 0.0873^2)$
$v_i^{\theta,gyr}$	$N(0,\ 0.0873^2)$

In the following, we omit i to simplify the expression. $\boldsymbol{M}(=[M_x\ M_y\ M_z]^{\mathrm{T}})$ is defined as magnetic sensor values, and $x,\ y,\ z$ are corresponding to three dimensional axes. $\boldsymbol{M}_{\mathrm{H}}(=[M_{Hx}\ M_{Hy}\ M_U]^{\mathrm{T}})$ is defined by the projection of $\boldsymbol{M}$ onto the horizontal plane. The coordinate transformation from $\boldsymbol{M}$ to $\boldsymbol{M}_{\mathrm{H}}$ is shown below.

$$\boldsymbol{M}_H = \boldsymbol{R}_y(\theta)\boldsymbol{R}_x(\phi)\boldsymbol{M} \tag{10}$$

$$\boldsymbol{R}_y(\theta) = \begin{bmatrix}\cos\theta & 0 & \sin\theta\\ 0 & 1 & 0\\ -\sin\theta & 0 & \cos\theta\end{bmatrix} \tag{11}$$

$$\boldsymbol{R}_x(\phi) = \begin{bmatrix}1 & 0 & 0\\ 0 & \cos\phi & -\sin\phi\\ 0 & \sin\phi & \cos\phi\end{bmatrix} \tag{12}$$

From (10), M_{Hx} and M_{Hy} can be calculated as follows.

$$M_{Hx} = M_x\cos\theta + M_y\sin\theta\sin\phi + M_z\sin\theta\cos\phi \tag{13}$$

$$M_{Hy} = M_y\cos\phi - M_z\sin\phi \tag{14}$$

Therefore, we express ψ_k^{mag} as follows.

$$\psi_k^{mag} = \begin{cases} 2\pi - \arctan(\frac{M_{k,Hx}}{M_{k,Hy}}) & (M_{k,Hx} > 0,\ M_{k,Hy} > 0)\\ -\arctan(\frac{M_{k,Hx}}{M_{k,Hy}}) & (M_{k,Hx} < 0,\ M_{k,Hy} > 0)\\ \pi - \arctan(\frac{M_{k,Hx}}{M_{k,Hy}}) & (M_{k,Hx} < 0,\ M_{k,Hy} < 0)\\ \pi - \arctan(\frac{M_{k,Hx}}{M_{k,Hy}}) & (M_{k,Hx} > 0,\ M_{k,Hy} < 0)\end{cases} \tag{15}$$

ψ_k^{mag} is calculated differently for each quadrant shown by $M_{k,x}$ and $M_{k,y}$. Since the clockwise direction of the azimuth angle is positive, the calculation method differs for each quadrant. ψ_k^{mag} is a value called the magnetic azimuth, and it is necessary to consider the declination that varies depending on the location. Therefore, in practice, the declination is subtracted from the calculated magnetic azimuth ψ_k^{mag}. Also, Hard-iron and Soft-iron effect are not considered in this paper.

III. GNSS/PDR INTEGRATED NAVIGATION

GNSS/PDR integrated navigation is realized by extended Kalman filter (EKF) [17], in this study. If the accuracy of the satellite positioning is good, EKF is performed. The state-space model for EKF can be expressed as follows.

$$\begin{bmatrix}e_{k+1}\\ n_{k+1}\\ \alpha_{k+1}\\ \beta_{k+1}\\ \gamma_{k+1}\end{bmatrix} = \begin{bmatrix}e_k + (\beta_k + \gamma_k f_k)\sin(\psi_k^{mag} + \alpha_k)\\ n_k + (\beta_k + \gamma_k f_k)\cos(\psi_k^{mag} + \alpha_k)\\ \alpha_k\\ \beta_k\\ \gamma_k\end{bmatrix} + \begin{bmatrix}w_k^e\\ w_k^n\\ w_k^{\alpha}\\ w_k^{\beta}\\ w_k^{\gamma}\end{bmatrix} \tag{16}$$

$$\begin{bmatrix}e_k^G\\ n_k^G\\ \tilde{\psi}_k\\ s_k^G\end{bmatrix} = \begin{bmatrix}1 & 0 & 0 & 0 & 0\\ 0 & 1 & 0 & 0 & 0\\ 0 & 0 & 1 & 0 & 0\\ 0 & 0 & 0 & f_k & f_k^2\end{bmatrix}\begin{bmatrix}e_k\\ n_k\\ \alpha_k\\ \beta_k\\ \gamma_k\end{bmatrix} + \begin{bmatrix}v_k^e\\ v_k^n\\ v_k^{\psi}\\ v_k^s\end{bmatrix} \tag{17}$$

where $e_k^G,\ n_k^G$ are the pedestrian's position of E-N plane by using the satellite positioning, s_k^G is the pedestrian's speed by using the satellite positioning. The noises $w_k^e,\ w_k^n,\ w_k^{\alpha},\ w_k^{\beta},\ w_k^{\gamma},\ v_k^e,\ v_k^n\ v_k^{\psi}\ v_k^s$ are assumed to be zero mean Gaussian white noise. From (7), the heading angle obtained from the satellite positioning ψ_k^G can be modeled as

$$\psi_k^G = \psi_k + v_k^{\psi} \tag{18}$$

$$= \psi_k^{mag} + \alpha_k + v_k^{\psi} \tag{19}$$

Therefore, the component $\tilde{\psi}_k$ in (17) is obtained as follows.

$$\tilde{\psi}_k = \psi_k^G - \psi_k^{mag} \tag{20}$$

e_k^G and n_k^G are calculated with reference to [19]. The distribution of each noise is experimentally designated as Table II.

TABLE II
NOISE DISTRIBUTIONS OF POSITIONING ESTIMATION

w_k^e	$N(0,\ 1^2)$
w_k^n	$N(0,\ 1^2)$
w_k^α	0
w_k^β	0
w_k^γ	0
v_k^e	$N(0,\ 3^2)$
v_k^n	$N(0,\ 3^2)$
v_k^ψ	$N(0,\ 0.8727^2)$
v_k^s	$N(0,\ 1^2)$

The initial value of the error covariance matrix $\boldsymbol{P}_0$ is experimentally determined as follows.

$$\boldsymbol{P}_0 = \begin{bmatrix} 1 & 0 & 0 & 0 & 0 \\ 0 & 1 & 0 & 0 & 0 \\ 0 & 0 & 0.1745^2 & 0 & 0 \\ 0 & 0 & 0 & 0.01 & 0 \\ 0 & 0 & 0 & 0 & 0.1 \end{bmatrix} \tag{21}$$

GNSS/PDR integrated navigation and estimating the parameters for a pedestrian are realized by executing this EKF step by step.

IV. PROPOSED METHOD

Fig. 3 shows the flowchart of proposed method. The satellite positioning has a condition that four or more satellites must be observed. We focus on the number of observable satellites. Furthermore, we focus on $\mathrm{C/N_0}$ (Carrier to Noise density ratio), which represents signal strength.

First, the walking detection is performed for each sampling. When a step is detected, the quality of the satellite positioning at that time is evaluated by the number of observable GPS and signal strength. If the conditions for the quality of satellite positioning are satisfied, positioning based on satellite positioning is performed and estimating the parameters of PDR. If the conditions are not satisfied, positioning is performed by PDR using the parameters estimated so far. When a step is detected, the pedestrian position is updated by one of the methods.

V. RESULTS

We verified the accuracy of the proposed method. In this paper, we utilized Android API (LocationManager) [20] as the satellite positioning. The location information by Android API is based on the satellite positioning, but it is also calculated comprehensively by using information such as Wi-Fi, Bluetooth, and so on. LocationManager is commonly used in application development in Android OS.

In the proposed method, positioning methods are switched according to environmental changes such as indoors and outdoors. Therefore, the experimenter moves seamlessly from outdoors to indoors and verify the positioning accuracy of the proposed method. We start the experiment from outdoors to estimate the parameters used in PDR. The timing of entering from outdoors to indoors (or from indoors to outdoors) is judged from the number of observable GPS and signal strength. If it is judged to be indoors, positioning is continued by PDR using the parameters estimated up to that point. The experimental conditions are summarized in Table III.

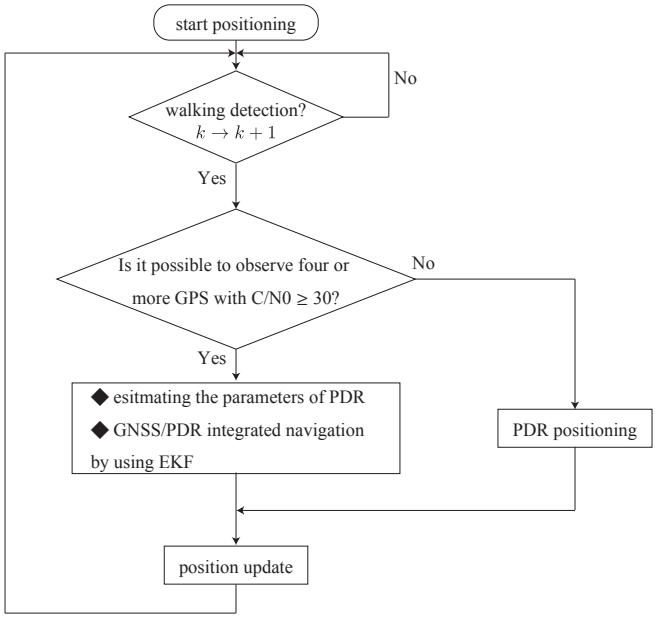

Fig. 3. Flowchart

TABLE III
EXPERIMENTAL CONDITIONS

Location	Ritsumeikan University (BKC)
Time (JS)	2023/05/15 13:32'55"–13:37'16"
Integrate system	Android API (LocationManager)
How to hold	texting
Initial value	$e_0 = 0,\ n_0 = 0,$ $\alpha_0 = 0,\ \beta_0 = -0.05,\ \gamma_0 = 0.45$

e_0 and n_0 are 0 because the starting point is defined as the origin. α_0 is set to 0 because the initial state of the smartphone is unknown. $\beta_0,\ \gamma_0$ are set according to [18].

The positioning result is shown in Fig. 4. The blue plot is the position information obtained by the Android API, and the red plot is the position estimated by the proposed method. We can see that the accuracy of the Android API is poor because the user is indoors from ② to ⑤ in Fig. 4. Also, it can be seen that the proposed method is strongly influenced by the location information of the Android API outdoors. In PDR, the longer the positioning time, the larger the error, so it can be said that it is appropriate to rely on the value of the satellite positioning.

Fig. 5 shows the number of observable GPS with a $\mathrm{C/N_0}$ of 30 or greater. The red line represents three GPSs. A and B are excerpts of the timings below four GPSs. The period between A and B in Fig. 5, there were less than four satellites. Also, the positions at A and B are plotted in Fig. 6. From these, it can be seen that the number of GPS is decreasing indoors and the positioning system is switched from the satellite positioning to PDR.

The estimates of α, β, and γ are shown in Fig. 7 - 9. In these figures, the horizontal axis represents the number of steps. If there are less than four GPSs, the estimate of each parameter holds its previous value. The change of α in Fig. 7 seems to be caused by the change in the smartphone attitude is seen. It can be seen that the parameter γ representing the correlation with the walking frequency f_k converges to a specific value. Since γ fluctuates a lot, you can see that β

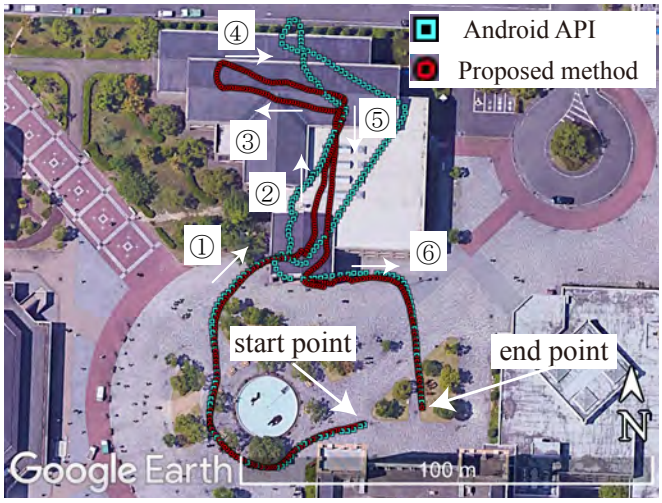

Fig. 4. Positioning result

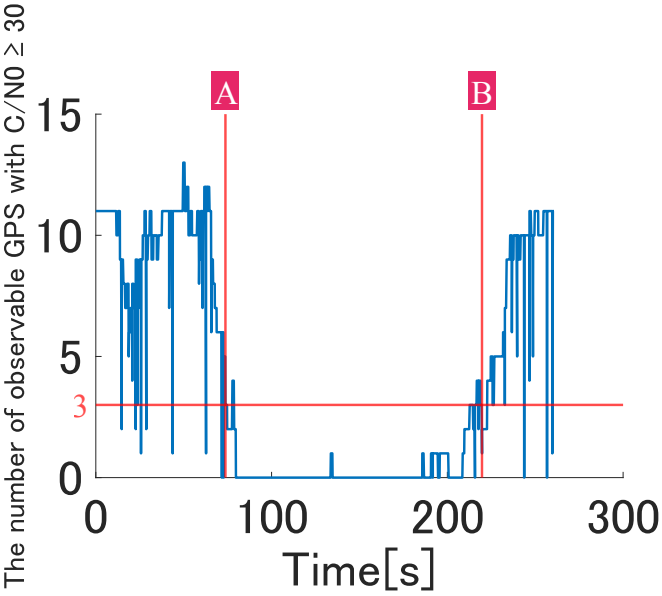

Fig. 5. Number of GPS satellites utilized

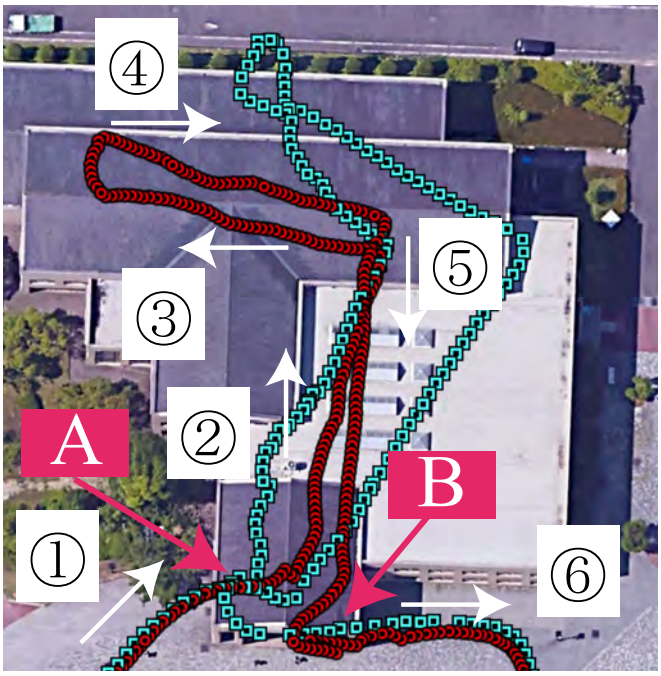

Fig. 6. Positioning result (zoomed)

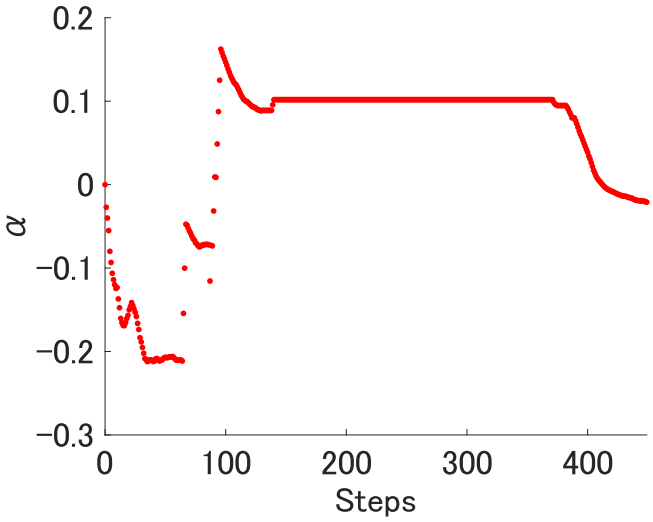

Fig. 7. Estimates of α

fluctuates slightly as well.

Fig. 10 shows the norm of acceleration used in the walking detection. The red circle is the local maxima and the green circle is the local minima. Such periodic outputs are produced by walking motions. Fig. 11 shows how the false walking detection system works. It can be seen that inappropriate extreme values can be removed. It was verified that even with the waveform shown in Fig. 11, walking was detected appropriately. The local minima nearest to the local maxima is used for walking detection.

VI. Conclusion

We proposed the GNSS/PDR integrated system which can efficiently take into account the characteristics of the walking motion and how the pedestrian holds for individual pedestrian. As a result, we can see the proposed method can estimate stride length and heading angle. We were able to obtain more accurate location information than the Android API, which is actually widely used on the Android OS.

References

[1] A. Makki, A. Siddig, M. Saad and C. Bleakley, "Survey of WiFi positioning using time-based techniques," *Computer Networks*, vol. 88, pp. 218–233, 2015.

[2] R. Faragher and H. Robert, "An analysis of the accuracy of bluetooth low energy for indoor positioning applications," *Proceedings of the 27th International Technical Meeting of The Satellite Division of the Institute of Navigation (ION GNSS+ 2014)*, Tampa, Florida, pp. 201–210, September 2014.

[3] X. Hou and J. Bergmann, "Pedestrian Dead Reckoning With Wearable Sensors: A Systematic Review,", *IEEE Sensors Journal*, vol. 21, no. 1, pp. 143–152, 2020.

[4] W. Kang and Y. HAN, "SmartPDR: Smartphone-based pedestrian dead reckoning for indoor localization,", *IEEE Sensors Journal*, vol. 15, pp. 2906–2916, 2014.

[5] Q. Zeng, J. Wang, Q. Meng, X. Zhang and S. Zeng, "Seamless Pedestrian Navigation Methodology Optimized for Indoor/Outdoor Detection,", *IEEE Sensors Journal*, vol. 18, no. 1, pp. 363–374, 2017.

[6] H. Weinberg, "Using the ADXL202 in pedometer and personal navigation applications,", *Analog Devices AN-602 application note*, vol. 2, no. 2, pp. 1–6, 2002.

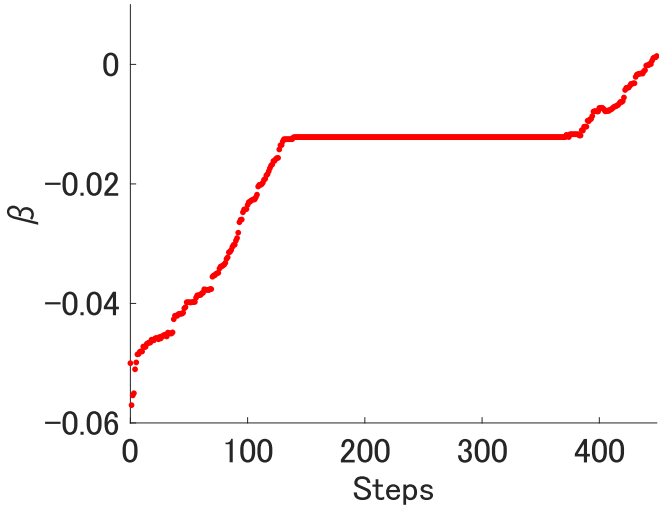

Fig. 8. Estimates of β

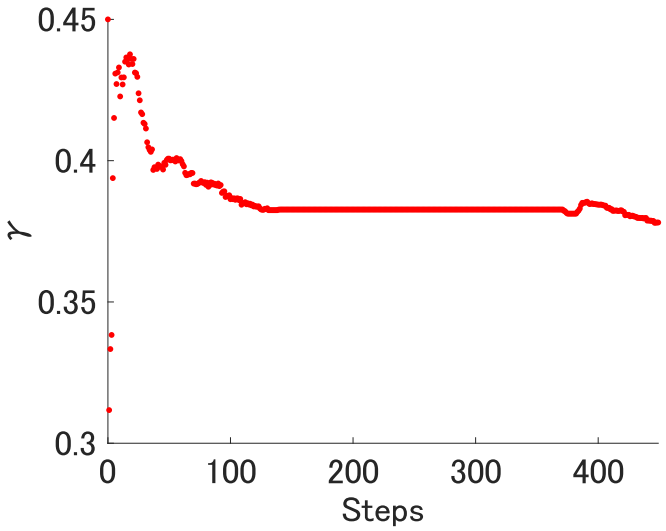

Fig. 9. Estimates of γ

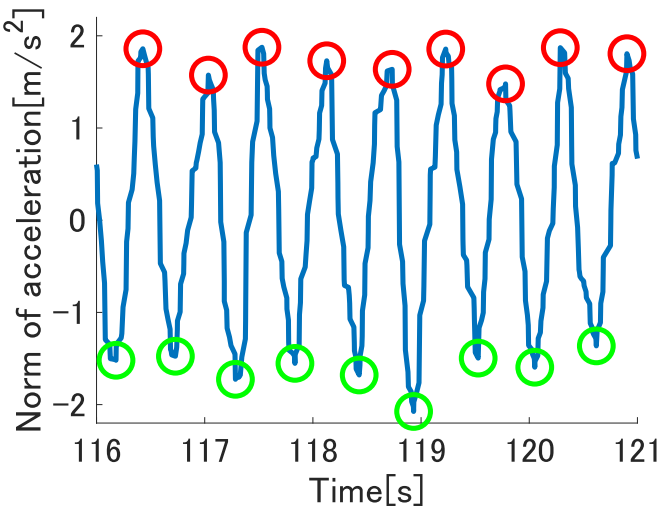

Fig. 10. Change in the norm of acceleration

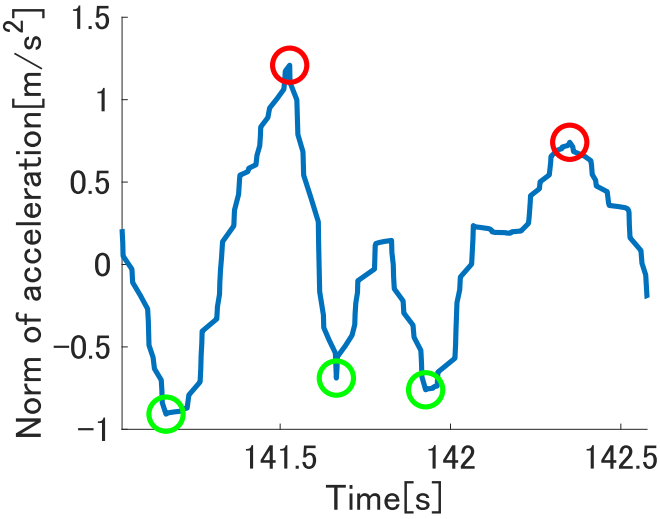

Fig. 11. False walking detection

[7] J. W. Kim, H. J. Jang, D.-H. Hwang and C. Park, "A step, stride and heading determination for the pedestrian navigation system,", *Journal of Global Positioning Systems*, vol. 3, no. 1-2, pp. 273–279, 2004.

[8] J. Scarlett, "Enhancing the performance of pedometers using a single accelerometer,", *Application Note, Analog Devices*, vol. 41, 2007.

[9] A. Rehman, H. Shahid, M. Afzal and H. Bhatti, "Accurate and direct GNSS/PDR integration using extended Kalman filter for pedestrian smartphone navigation,", *Gyroscopy and Navigation*, vol. 11, no. 2, pp. 124–137, 2020.

[10] R. Jirawimut, P. Ptasinski, V. Garaj, F. Cecelja and W. Balachandran, "A method for dead reckoning parameter correction in pedestrian navigation system,", *IEEE Transactions on Instrumentation and Measurement*, vol. 52, pp. 209–215, 2003.

[11] C. Jiang, Y. Chen, C. Chen, J. Jia, H. Sun, T. Wang and J. Hyyppa, "Implementation and performance analysis of the PDR/GNSS integration on a smartphone,", *GPS Solutions*, vol. 26, pp. 81, 2022.

[12] C. Jiang, Y. Chen, C. Chen, S. Chen, Q. Meng, Y. Bo and J. Hyyppa, "Cooperative Smartphone GNSS/PDR for Pedestrian Navigation,", *IEEE Transactions on Circuits and Systems II: Express Briefs*, 2022.

[13] L. T. Hsu, Y. Gu, Y. Huang and S. Kamijo, "Urban pedestrian navigation using smartphone-based dead reckoning and 3-D map-aided GNSS,", *IEEE Sensors Journal*, vol. 16, pp. 1281-1293, 2015.

[14] D. M. Bevly and S. Cobb, "GNSS for VEHICLE CONTROL,", *Artech House*, 2010.

[15] S. Liuyang, P. Chen and H. Wang, "Intelligent diagnosis method using probability density distribution and principal component analysis - Application on gear rotating machinery," *2016 International Symposium on Flexible Automation (ISFA)*, 2016

[16] J. Racko, P. Brida, A. Perttula, J. Parviainen and J. Collin, "Pedestrian Dead Reckoning with Particle Filter for Handheld Smartphone,", *Indoor Positioning and Indoor Navigation (IPIN)*, pp. 1-7, 2016.

[17] M. S. Grewal and A. P. Andrews, "Kalman Filtering Theory and Practice Using MATLAB Second Edition,", *A Wiley-Interscience Publication*, 2001.

[18] S. Shin, C. Park, J. Kim, H. Hong and J. Lee, "Adaptive Step Length Estimation Algorithm Using Low-Cost MEMS Inertial Sensors,", *IEEE sensors applications symposium*, pp. 1-5, 2007.

[19] S. P. Drake, "Converting GPS coordinates [phi, Lambda, h] to navigation coordinates (ENU),", Australian Government Dept. Def., Canberra, BC, Australia, Tech. Note, DSTO-TN-0432, 2002.

[20] "Android Developer", https://developer.android.com, accessed on Feb.7, 2022.